Available online at www.sciencedirect.com

ScienceDirect

Biomedical Journal

journal homepage: www.elsevier.com/locate/bj

Original Article

Regulation of endothelial cell arrangements within hMSC – HUVEC co-cultured aggregates

Anthony J. Deegan [a], *Wim J. Hendrikson* [b], *Alicia J. El Haj* [a], *Jeroen Rouwkema* [c], *Ying Yang* [a,*]

[a] *Institute for Science and Technology in Medicine, School of Medicine, Keele University, Stoke-on-Trent, United Kingdom*

[b] *Department of Tissue Regeneration, MIRA Institute for Biomedical Technology and Technical Medicine, University of Twente, Enschede, AE, the Netherlands*

[c] *Department of Biomechanical Engineering, Technical Medical Centre, University of Twente, Enschede, the Netherlands*

ARTICLE INFO

Article history:
Received 3 April 2018
Accepted 14 January 2019
Available online 17 July 2019

Keywords:
Co-culture
Cellular aggregation
Pre-vascularisation
Mesenchymal stem cell
HUVEC

ABSTRACT

Background: Micro-mass culturing or cellular aggregation is an effective method used to form mineralised bone tissue. Poor core cell viability, however, is often an impeding characteristic of large micro-mass cultures, and equally for large tissue-engineered bone grafts. Because of this, efforts are being made to enhance large graft perfusion, often through pre-vascularisation, which involves the co-culture of endothelial cells and bone cells or stem cells.

Methods: This study investigated the effects of different aggregation techniques and culture conditions on endothelial cell arrangements in mesenchymal stem cell and human umbilical vein endothelial cell co-cultured aggregates when endothelial cells constituted just 5%. Two different cellular aggregation techniques, i.e. suspension culture aggregation and pellet culture aggregation, were applied alongside two subsequent culturing techniques, i.e. hydrostatic loading and static culturing. Endothelial cell arrangements were assessed under such conditions to indicate potential pre-vascularisation.

Results: Our study found that the suspension culture aggregates cultured under hydrostatic loading offered the best environment for enhanced endothelial cell regional arrangements, closely followed by the pellet culture aggregates cultured under hydrostatic loading, the suspension culture aggregates cultured under static conditions, and the pellet culture aggregates cultured under static conditions.

Conclusions: The combination of particular aggregation techniques with dynamic culturing conditions appeared to have a synergistic effect on the cellular arrangements within the co-cultured aggregates.

* *Corresponding author*. Institute for Science and Technology in Medicine, School of Medicine, Keele University, Stoke on Trent, ST4 7QB, United Kingdom.
E-mail address: y.yang@keele.ac.uk (Y. Yang).

Peer review under responsibility of Chang Gung University.
https://doi.org/10.1016/j.bj.2019.01.003

At a glance of commentary

Scientific background on the subject

The enhanced perfusion of tissue-engineered constructs through pre-vascularisation is a plausible solution to improve the cell viability and integration of large tissue-engineered graft products to host. Co-culturing of endothelial cells and mesenchymal stem cells and regulation of the spatial arrangement of endothelial cells could achieve potential pre-vascularisation.

What this study adds to the field

In a micro-mass culturing or cellular aggregation model, new protocols for MSC and HUVEC co-cultured aggregates have been established, which could achieve higher spatially arranged cellular structure resembling pre-vascularisation through aggregate formation techniques and subsequent culture conditions even for the presence of only 5% endothelial cells.

Large tissue-engineered bone grafts often suffer from poor core cell viability which subsequently leads to compromised graft integration and possible graft failure [1]. Such an inhibition to the viability of implants poses a major obstacle to the progression and translation of tissue engineering [2]. With this in mind, the enhanced perfusion of tissue-engineered constructs through pre-vascularisation has been proposed as a plausible solution with numerous routes currently being explored to refine and enhance current bone tissue engineering techniques [3,4]. The intent of this study was to evaluate the potential effects of a number of experimental parameters with a focus on cellular arrangement as an indicator for potential pre-vascularisation.

The first of several parameters being used here involves the co-culturing of two specific cell types, i.e. human umbilical vein endothelial cells (HUVEC) and mesenchymal stem cells (MSC). Previous studies have used endothelial cells (EC) in conjunction with various other cell types in an attempt to achieve *in vitro* pre-vascularisation within scaffold constructs [5–8], the relative success of which inspired the use of ECs here. MSCs too are being used here in conjunction with HUVECs. MSCs have been shown to enhance angiogenesis in a number of studies [9–11] and have also been seen to enhance tumour growth through an increase in the secretion of proangiogenic factors and enhanced blood vessel formation [12]. The co-transplantation of endothelial progenitor cells (EPC) and MSCs has also been shown to promote neovascularisation and bone regeneration within a rat calvarium model [13]. Their proangiogenic properties are, therefore, hoped to positively influence HUVEC arrangement into viable pre-vascular structures here. MSCs from various sources have also been used extensively in numerous studies as osteogenic precursors [14–17]. With large bone graft viability being the motivation behind this study, the decision was made to use an osteogenic-supplemented medium to guide the MSCs towards an osteogenic lineage in an attempt to replicate conventional bone tissue engineering practices; however, osteogenesis itself was not a topic of investigation here.

Another parameter being examined is the environment within which such co-cultures are developed. Numerous studies have shown that the use of three-dimensional (3D) microenvironments offer the ideal setting for improved cell – cell communications through enhanced cell – cell signalling, proliferation, differentiation and survival [18,19]. In addition, implanting MSCs in aggregate form would appear to enhance the stimulation of angiogenesis and neovascularisation, with such a technique working well for implants of a smaller size or when used as a supportive role for osteogenesis [2]. Co-culturing in this way, therefore, makes for a logical choice within this study. One further aspect of aggregate culturing to be considered here is what influences might the specific aggregation method hold over potential pre-vascularisation-like cellular arrangements. There are a plethora of proven techniques available, and to date, the author is unaware of any study that has actually compared aggregation techniques for cellular arrangement or vascularisation potential. Furthermore, it is thought that unmodified MSCs alone may not be sufficient for supporting vascularisation in large grafts [2]; additional environmental conditions may be required to further enhance the positive results seen thus far. Fortunately, the use of bioreactors is thought to offer such environmental conditions needed for advanced tissue engineering [20].

Under normal physiological conditions, loading placed on the bone through compression and/or tension via movement drives interstitial fluid flow through the lacunae of the bone resulting in the application of fluid sheer stresses [21], which are detectable by the cells [22–25]. Such mechanical stimuli are known to influence embryonic bone formation [26,27] as well as post-embryonic bone regeneration [28]. Here, we intend to replicate the effects of a uniformly distributed stimulus throughout the aggregate body, and so opted to replace direct mechanical deformation via compression/tension with an indirect approach, i.e. hydrostatic loading. Such an approach has been used previously as a stimulus for directing cell fate within various tissues, such as the intervertebral disc, the vascular system, articular cartilage and bone [20,29,30]. The use of a hydrostatic bioreactor is appealing because the application of hydrostatic loading to a tissue-engineered construct is thought to not only provide physical forces, but to also increase the transfer of small molecules, such as O_2 and CO_2, into the tissue matrix [31]. pH levels and dissolved O_2 concentrations have been shown in numerous studies to influence cellular mechanisms, such as inter-cellular signalling, cell proliferation and differentiation [32,33], as well as the cell cycle, apoptosis and protein synthesis [34–39].

The current study aimed to use the above-mentioned techniques in an attempt to contribute to the ongoing discussions centred around one very important question: how might current tissue engineering protocols be utilised and refined to enhance perfusion within cellular aggregates for improved large graft survival rates? To do this, the aim of the study was to introduce and compare two different aggregation methods, i.e. suspension culture and pellet culture methods,

and two different culture conditions, i.e. hydrostatic loading and static culturing, on 3D MSC – HUVEC co-cultured aggregate constructs with the goal of offering the best HUVEC spatial organisation representing potential pre-vascularisation within an *in vitro* setting.

Materials and methods

Cell culturing

Human MSCs and HUVECs were used in this study. Human MSCs were isolated from commercially-acquired bone marrow mononuclear cells (MNC) (Lonza, Belgium) using a conventional attachment isolation protocol (adapted from D'Ippolito et al. [40]). The MSCs were cultured using proliferative/basal medium consisting of low glucose (1 g/l) Dulbecco's Modified Eagle Medium (DMEM) (Lonza, Belgium), 10% foetal bovine serum (FBS) (Lonza, Belgium), 1% antibiotic-antimycotic solution (A + A) (Sigma–Aldrich, UK), 1% non-essential amino acids (NEAA) (Sigma–Aldrich, UK) and 2 mM l-glutamine (Lonza, Belgium). The cells were maintained at 37 °C and 5% CO_2, and were used for experiments at passage 4. The HUVECs (Life Technologies, UK) were cultured using Medium 200 (Life Technologies, UK) supplemented with 2% low serum growth supplement (LSGS) (Life Technologies, UK) at 37 °C and 5% CO_2 [41]. The cells were used at passage 4.

Cell aggregation

Prior to aggregation, the HUVECs were tagged with a membrane dye, PKH fluorescent cell linker kit (Sigma–Aldrich, UK), to allow for their tracking during culturing. The HUVECs were labelled following the manufacturer's protocol. Once ready, both MSCs and HUVECs were aggregated together using two different techniques for comparative purposes. The first aggregation technique involved the formation of aggregates on a standard suspension culture plate (Sarstedt, UK) coated with a Pluronic F127 solution (BASF, UK) (denoted as suspension culture aggregation) [42]. To create the coated suspension culture plate, 500 μl of a sterile 2% Pluronic F127 solution (in dH_2O) was added to each of the wells of a 24-well suspension culture plate and incubated at room temperature for 24 hours. The remaining solution was removed and each well was seeded with 1×10^5 cells in 1 ml proliferative medium. The second aggregation technique involved the centrifugation of cells into cell pellets (denoted as pellet culture aggregation). One x 10^5 cells were added in 1 ml proliferative medium to a 1.5 ml micro-centrifuge tube. The cells were then centrifuged for 4 minutes at 168×*g* (1000 rpm) before being placed in an incubator at 37 °C and 5% CO_2.

Both aggregation techniques used 1×10^5 cells/aggregate. Aggregates consisted of a co-culture of 95% MSCs and 5% HUVECs [43]. Regardless of aggregation technique, the MSC/HUVEC aggregates were formed using MSC proliferative medium and HUVEC basal medium at a ratio of 1:1 (adapted from Saleh et al. [44]). All aggregates were cultured for 48 hours before being encapsulated in collagen hydrogel.

Collagen encapsulation

Collagen encapsulation via rat tail type 1 collagen (BD Biosciences, UK) was used to house the aggregates during the hydrostatic loading and static culturing phase of the study. Post-aggregation, the individual aggregates were placed into individual wells of a standard 24-well tissue culture polystyrene (TCP) plate (Greiner, UK). The aggregates were centred within the wells and any remaining medium was removed immediately prior to encapsulation. The collagen gel was then formed with a concentration of 3 mg/ml using the manufacturer's protocol. One ml collagen gel was added to each well. The gel/aggregate constructs were then placed in an incubator at 37 °C and 5% CO_2 for 20 minutes to allow for the gel to set. Once set, each well received 1 ml medium consisting of osteogenic-supplemented medium (i.e. MSC basal medium supplemented with dexamethasone (10 nM) (Sigma–Aldrich, UK), ascorbic acid (50 μg/ml) (Sigma–Aldrich, UK) and β-glycerophosphate (10 mM) (Sigma–Aldrich, UK)) and HUVEC basal medium at a ratio of 1:1. The aggregates were then cultured for 24 hours before entering the next phase of the study.

Aggregate culturing

The next phase of the study involved two different culture environments: hydrostatic (denoted as loaded) and static (denoted as static). Twenty-four hours following collagen encapsulation, the loaded samples were subjected to their first loading session. The hydrostatic chamber was sterilised before use via autoclaving. The well plate was placed inside the chamber with the plate lid removed. The lid of the chamber was then bolted in place before the chamber was connected to the pressure generator. The whole chamber was then placed inside an incubator set to 37 °C and 5% CO_2. Loading was carried out for 1 hour every 24 hours for 7–10 days post-collagen encapsulation at a pressure of 280 kPa and a frequency of 1 Hz [30]. The aggregate constructs intended for static culturing were simply kept in an incubator at 37 °C and 5% CO_2 for the remaining duration of the experiment (7–10 days). After 7–10 days of loaded and/or static culturing, the aggregate samples were terminated. Those samples intended for cryosectioning and immunohistochemical staining were not fixed until after they were sectioned.

Imaging

Optical imaging for monitoring aggregate size was carried out on a minimum of three samples per variable at 10X magnification (Olympus CKX41). Post-collagen encapsulation, imaging of the aggregates took place immediately and again every 3–4 days to monitor cellular outgrowth from both culture conditions. Epifluorescent and brightfield imaging for immunohistochemical staining and whole aggregate monitoring was carried out at 10X magnification after 3, 7 and 10 days of loaded and/or static culturing post-collagen encapsulation (Nikon Eclipse Ti microscope). Confocal z-stacking was intended to monitor inner-aggregate cellular arrangements through the imaging of membrane dye-tagged cells. Confocal z-stacking was carried out at 10X magnification 24 hours post-

collagen encapsulation and immediately prior to each loading session (Olympus IX83).

Aggregate measuring

Aggregate size was measured using optical images taken immediately after collagen encapsulation with at least three replicates per variable. The length and breadth of the aggregates were measured and an average (mean ± standard error of the mean) was taken from both to get the approximate aggregate size. Image J software was used to obtain each measurement and was calibrated separately for each image using the scale bars acquired from Image-Pro Insight software. The aspect ratio of each aggregate was acquired using the same images previously used for aggregate size measurements from measuring the aggregate length and breadth at their longest points. A ratio was then acquired with 1 representing a perfect circle. A higher aspect ratio indicated a more elongated or irregularly-shaped aggregate. Image J software was calibrated separately according to the images' scale bars for each image.

Cryosectioning

For the samples to be cryosectioned, they were snap-frozen in liquid nitrogen immediately prior to cryosectioning. The individual samples were placed on a glass slide and covered in an optimal cutting temperature (OCT) (Tissue-Tek, UK) compound. The OCT/aggregate samples were transferred to a sample holder and sectioned into 8 μm thick slices. The slices were collected on fresh glass slides which were then placed into a cylinder of cold acetone to fix the samples and remove the OCT compound.

Immunostaining

CD31 staining was used to identify the presence and spatial distribution of HUVECs located in and/or around the aggregates. The sample sections were incubated for 30 minutes in 10% FBS (diluted in phosphate buffered saline (PBS)) to prevent non-specific background staining (blocking). The samples were then incubated for 1 hour in the primary antibody, mouse anti-human CD31 (Dako, UK), at a dilution of 1:20 in PBS. The samples were then incubated for 1 hour in the secondary antibody, alexa-fluor 594-conjugated goat anti-mouse IgG1 (Life Technologies, UK), diluted 1:200 in PBS. DAPI staining was carried out using a DAPI-conjugated mounting medium without further adjustment. The samples were then ready for imaging.

Cellular distribution

The level of organised cellular arrangement was calculated using HUVEC distribution throughout the co-cultured cellular aggregates. HUVEC distribution was defined and quantified as the percentage of positive space within the aggregates imaged by confocal z-stacking with 5 μm increments to cover a depth range of 250 μm, where HUVECs appeared as bright subjects in greyscale images. A minimum of three samples were used per variable after 3 and 10 days of loaded and/or static culturing. Image J software was used to first apply a Bandpass Filter to the confocal images to enhance the visualisation of HUVEC distribution. From each sample, whole aggregate area was then measured using the contouring feature in Image J software, followed by the combined area of the inner-aggregate voids, again using the contouring feature ('voids' denotes the areas within the aggregate where HUVECs were not present). Subtracting the latter from the former gave the total area within each of the aggregates occupied by HUVECs. A percentage was then derived indicating the level of cellular organisation within the aggregates.

Statistical analysis

A minimum of three specimens were used for all image acquisition or quantitative measurements. A total of 7 independent experiments was carried out to complete this study with similar trends noted throughout. Recorded data was initially sorted using Microsoft Office Excel software before being transferred to GraphPad Prism for statistical analysis and graphing. Data were presented as a mean value ± standard error of the mean. Groups were compared using independent t-tests and one-way analysis of variance (ANOVA). A p-value below 0.05 was used to indicate statistical significance. In graphs, * signifies $p < 0.05$, and ** signifies $p < 0.01$.

Results

Aggregate formation

Both suspension and pellet aggregation techniques formed aggregates of different sizes and shapes despite these two techniques using the same cell numbers. Fig. 1 shows the average size of the aggregates immediately post-collagen encapsulation. The average suspension culture aggregate was 885 μm and the average pellet culture aggregate was 497 μm (t-test, $p = 0.0133$). Also shown is the average aspect ratio of the aggregates immediately post-collagen encapsulation. The suspension culture aggregates had an average aspect ratio of 1.23 and the pellet culture aggregates had an average aspect ratio of 1.102.

Optical imaging of the F127-coated suspension cultures over the 48-hour aggregation period showed multiple small aggregates being formed which subsequently combined together to form one large aggregate in each well. Alternatively, the pellet aggregation technique immediately formed one cell pellet which aggregated over the same 48-hour aggregation period (data not shown). The shape of the final suspension culture aggregates would also lead one to believe that the initial small aggregates of the suspension culture that eventually combined to formed single suspension culture aggregates were still present in the final aggregate form in many cases.

Cellular outgrowth

The first observation to be made over the course of the study concerned cellular outgrowth from the aggregates post-collagen encapsulation, i.e. cells migrating from the main aggregate bodies [Fig. 2]. Considerable cellular outgrowth was

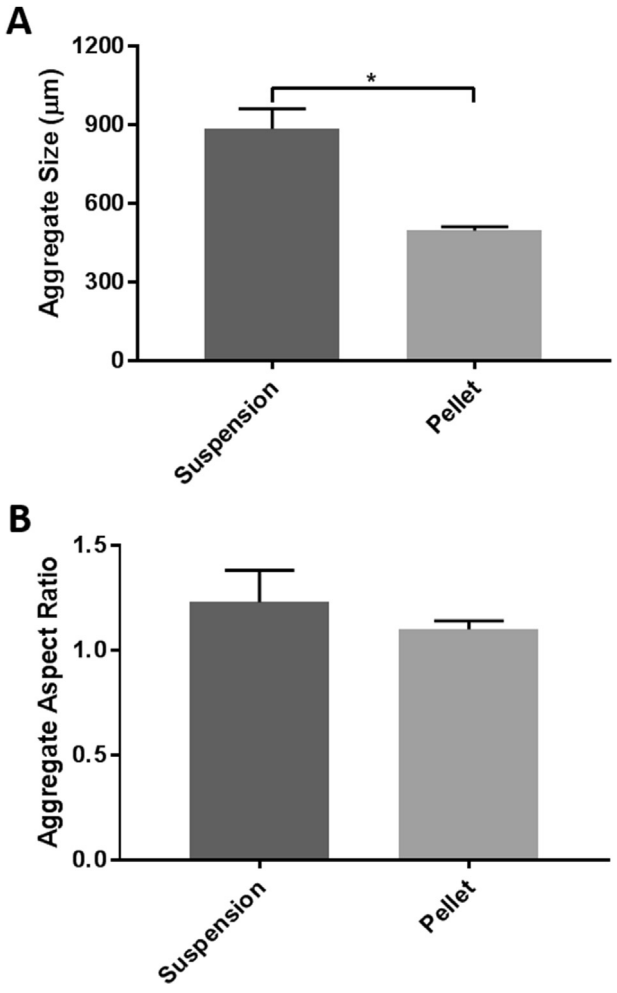

Fig. 1 Aggregate measurements comparing both aggregation techniques. **(A)** The average (mean) aggregate size. **(B)** The average (mean) aggregate aspect ratio. The aggregates were formed from both aggregation techniques immediately post-collagen encapsulation. Error bar represents standard error of the mean. * signifies $p < 0.05$.

noted from the brightfield and optical images taken of the aggregates with such outgrowth being particularly obvious from the static cultured samples, even from the early stages of the experiment. A considerably smaller volume of outgrowth was witnessed from the loaded samples. The extent of outgrowth from the static samples increased over time whereas the extent of outgrowth from the loaded samples appeared to remain constant. Measurements suggest that the average cellular outgrowth experienced by the aggregates under loaded conditions was approximately 10% of the original aggregate size, regardless of the aggregation technique used to initially develop the aggregates. The average cellular outgrowth experienced by the aggregates under static conditions was difficult to accurately measure as the outgrowth extended beyond the microscope's field of view, though it was thought to exceed 40% of the original aggregate size (data not shown). The level of outgrowth also corresponded with a change in aggregate colour density [Fig. 2]. That is, the aggregates that experienced a higher degree of outgrowth also experienced higher colour density loss.

Cell arrangements within the aggregates

Confocal z-stacking has given an insight into the cellular arrangements taking place within the whole aggregate samples [Figs. 3 and 4A]. Fig. 3 shows confocal images taken of the fluorescently-tagged HUVECs immediately post-collagen encapsulation. Even from this very early time point, considerable cellular arrangements can be distinguished. HUVEC arrangement within the suspension culture aggregates appeared to be regional, whilst the HUVECs present in the pellet culture aggregates were more uniformly distributed throughout the aggregate bodies.

As culturing continued, increased HUVEC arrangement was noted within the samples cultured under hydrostatic loading [Fig. 4A]. After 10 days of culturing post-collagen encapsulation, the samples undergoing loading were still showing increased HUVEC arrangement when compared to statically-cultured samples for both aggregate formation techniques. The loaded suspension culture aggregates have shown the most obvious cellular arrangements followed closely by the loaded pellet culture aggregates. The static suspension culture aggregates were also showing more cellular arrangement when compared to the static pellet culture aggregates.

Quantifying the level of cellular arrangement has shown a similar trend to that of visual observations [Fig. 4B]. After 3 days in culture, the loaded suspension culture aggregates had a HUVEC distribution of 66.11%, the loaded pellet culture aggregates had 78.49%, the static suspension aggregates had 75.95%, and the static pellet culture aggregates had 85.61%. Whilst these figures did not statistically differ, a trend was visible. After 10 days in culture, the loaded suspension culture aggregates had a HUVEC distribution of 58.14%, the loaded pellet culture aggregates had 71.91%, the static suspension aggregates had 81.62%, and the static pellet culture aggregates had 90.78%. Both of the loaded samples, suspension and pellet culture aggregates, differed significantly from their static counterparts (t-test, $p = 0.0054$ and 0.022, respectively). HUVEC distribution throughout the loaded suspension culture aggregates was also significantly lower than their static pellet culture aggregate counterparts (t-test, $p = 0.0012$). A one-way ANOVA also showed a significant difference across all four variables, with $p = 0.0009$. In addition, HUVEC distribution throughout both of the loaded samples can be seen to have decreased, whilst distribution throughout both of the static samples increased. The change in distribution trends from 3 to 10 days shows the influence hydrostatic loading had on HUVEC distribution.

CD31 staining of aggregate sections also showed a similar trend to previously conducted HUVEC tracking and confocal imaging [Fig. 5]. The loaded samples appeared to better maintain their initial spheroidal shape over the duration of the study, more so in the pellet culture aggregates. The static samples experienced sizeable cellular outgrowth and altered aggregate size and shape as a result. Particular HUVEC arrangements appeared more distinct also. The HUVECs would appear most organised in the loaded samples.

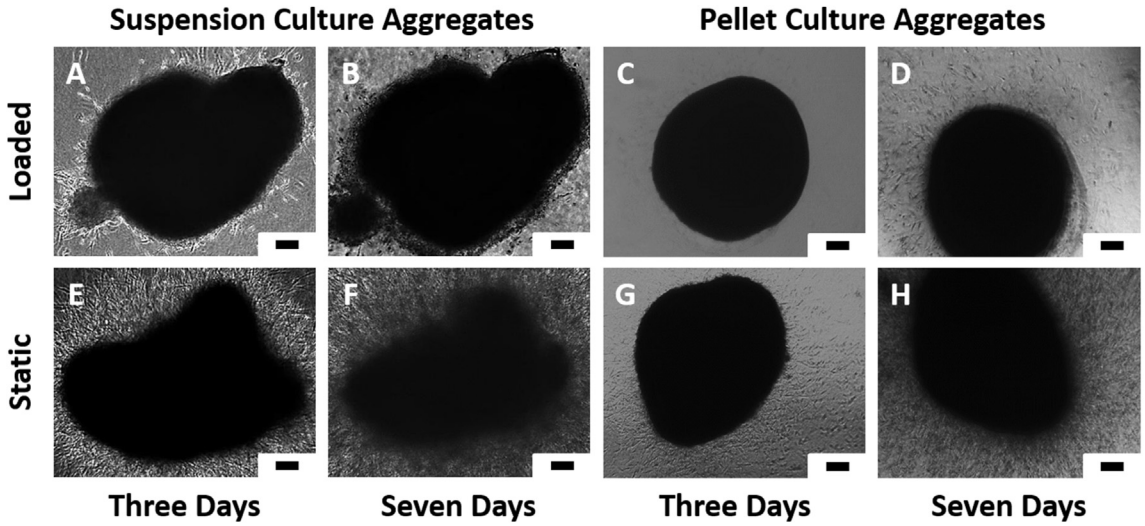

Fig. 2 Brightfield and optical images of MSC/HUVEC co-cultured aggregates post-collagen encapsulation at 10X magnification. (**A**) A suspension culture aggregate grown for 3 days in collagen under loaded conditions. (**B**) A suspension culture aggregate grown for 7 days in collagen under loaded conditions. (**C**) A pellet culture aggregate grown for 3 days in collagen under loaded conditions. (**D**) A pellet culture aggregate grown for 7 days in collagen under loaded conditions. (**E**) A suspension culture aggregate grown for 3 days in collagen under static conditions. (**F**) A suspension culture aggregate grown for 7 days in collagen under static conditions. (**G**) A pellet culture aggregate grown for 3 days in collagen under static conditions. (**H**) A pellet culture aggregate grown for 7 days in collagen under static conditions. Scale bar represents 100 μm.

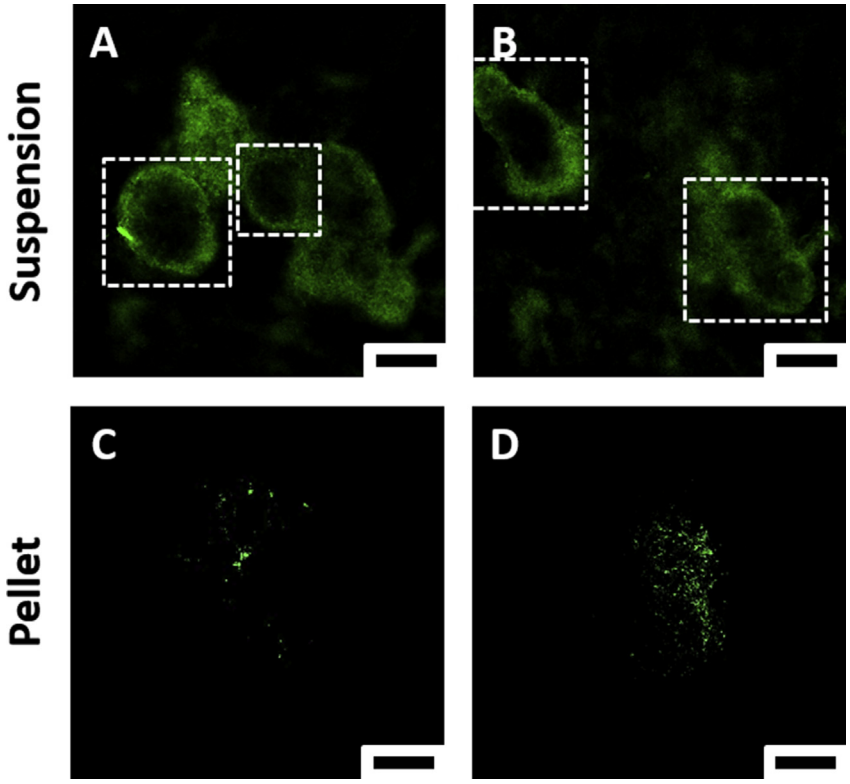

Fig. 3 Confocal images of fluorescently-tagged HUVECs in MSC/HUVEC co-cultured aggregates at 10X magnification. (**A**) and (**B**) Suspension culture aggregates. (**C**) and (**D**) Pellet culture aggregates. Images were taken immediately following collagen encapsulation (pre-loading). The MSCs were not fluorescently-tagged. White boxes highlight areas of compartmentalisation within the suspension culture aggregates. Scale bar represents 200 μm.

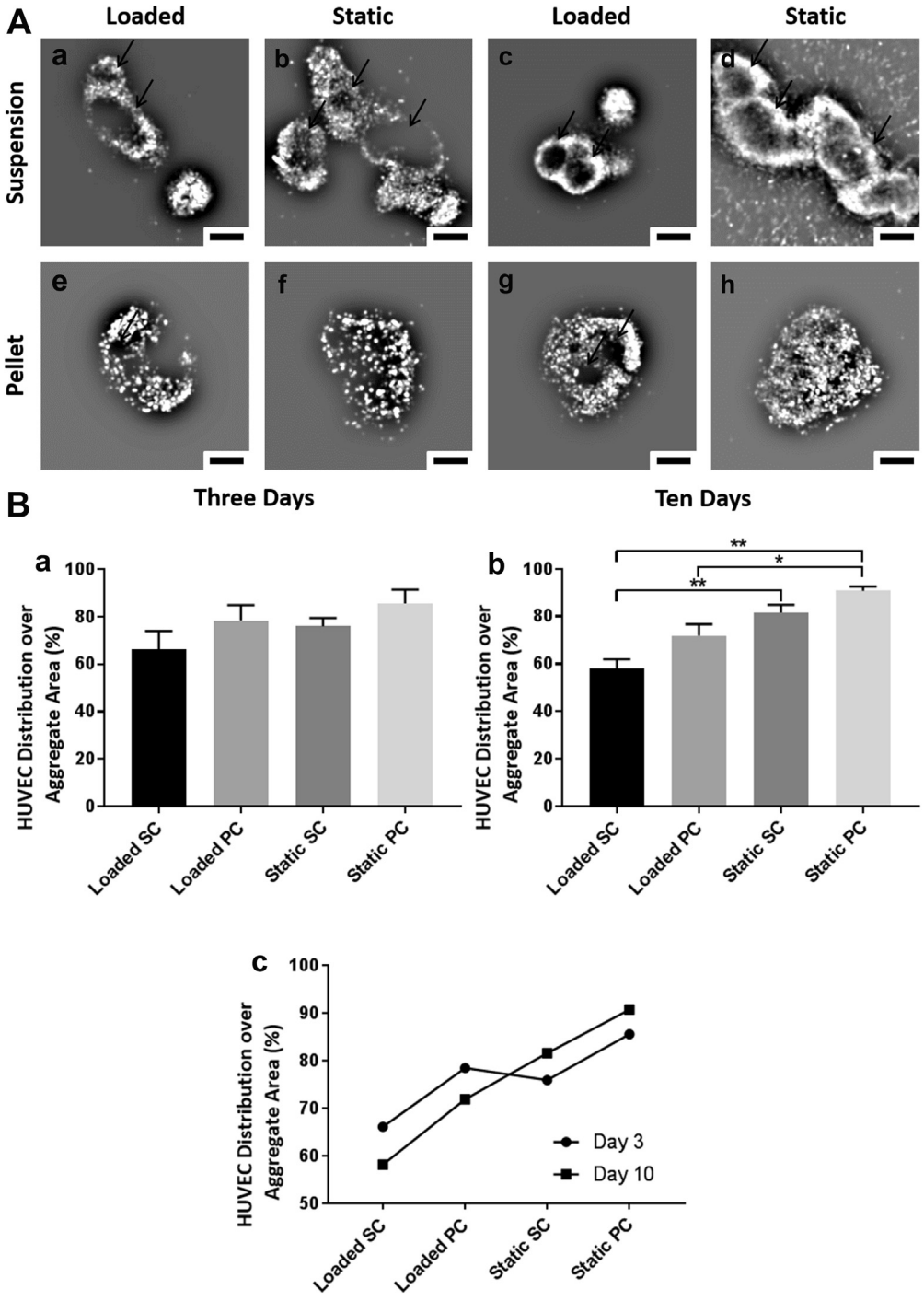

Fig. 4 **(A)** Confocal images of fluorescently-tagged HUVECs in MSC/HUVEC co-cultured aggregates at 10X magnification with a Bandpass Filter applied (converting to greyscale colour). **(a)** A loaded suspension aggregate cultured for 3 days in collagen. **(b)** A static suspension aggregate cultured for 3 days in collagen. **(c)** A loaded suspension aggregate cultured for 10 days in collagen. **(d)** A static suspension aggregate cultured for 10 days in collagen. **(e)** A loaded pellet aggregate cultured for 3 days in collagen. **(f)** A static pellet aggregate cultured for 3 days in collagen. **(g)** A loaded pellet aggregate cultured for 10 days in collagen. **(h)** A static pellet aggregate cultured for 10 days in collagen. Black arrows indicate areas of regional cellular arrangements. Scale bar represents 200 μm. **(B)** Semi-quantification of HUVEC distribution throughout the aggregates represented as a percentage of total aggregate area. **(a)** Suspension and pellet culture aggregates grown for 3 days in collagen under loaded and static conditions. **(b)** Suspension and pellet culture aggregates grown for 10 days in collagen under loaded and static conditions. **(c)** Comparison between HUVEC distribution trends within the suspension and pellet culture aggregates from both culture conditions over both 3 and 10 days post-collagen encapsulation. Abbreviation 'SC' refers to suspension culture aggregates, and abbreviation 'PC' refers to pellet culture aggregates. Error bar represents standard error of the mean. * signifies $p < 0.05$, ** signifies $p < 0.01$.

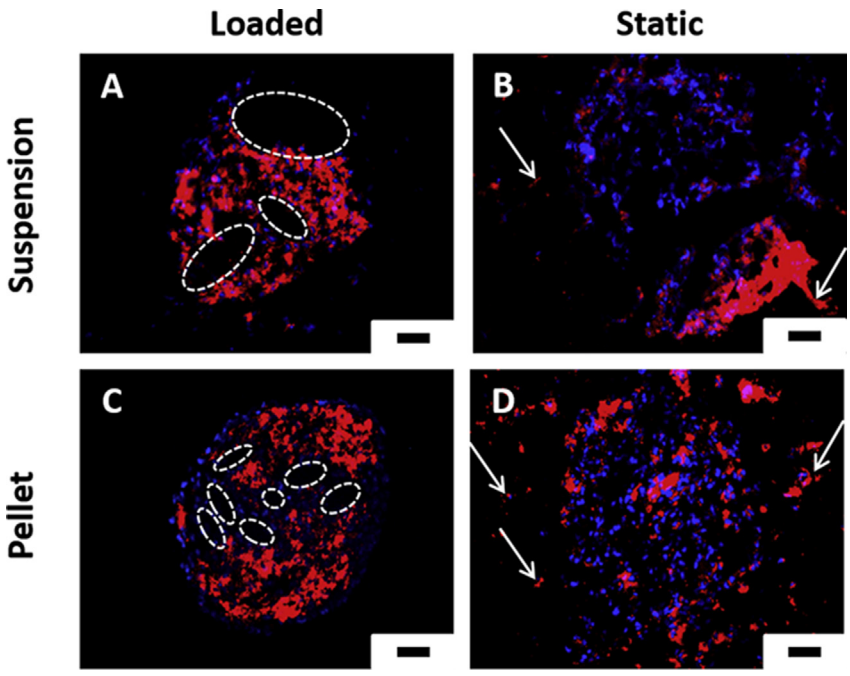

Fig. 5 Epifluorescent images of CD31-stained (red) MSC/HUVEC co-cultured aggregate sections at 10X magnification. (**A**) Suspension culture aggregate under loaded conditions. (**B**) Suspension culture aggregate under static conditions. (**C**) Pellet culture aggregate under loaded conditions. (**D**) Pellet culture aggregate under static conditions. Images were taken following 7 days in collagen under loaded and static culture conditions. The cells were counter stained by DAPI (blue). The white ellipses highlight areas within the aggregate bodies void of HUVECs, and thus, possible pre-vascularisation. The white arrows highlight examples of cellular outgrowth from the aggregate bodies. Scale bar represents 100 μm.

Discussion

The advantages of using 3D microenvironments (cellular aggregates) for tissue engineering has been discussed in previously published literature [45] with cellular aggregates having been previously employed for the study of vascularisation [44]. What is not immediately clear from previously conducted research, however, is whether the specific aggregation techniques and/or dynamic culture environments used will influence the extent to which the formed aggregate can be pre-vascularised or made to self-organise into ordered endothelial cell arrangements when EC cells are in minority. This study has evaluated a number of variables, such as the use of 3D microenvironments and dynamic culturing in combination with the use and comparison of two different aggregation techniques, in an attempt to answer the question noted above.

The aggregates used here consisted of MSC/HUVEC co-cultures that were formed using two different methods: suspension culture aggregation and pellet culture aggregation. The suspension culture method comprised a simple F127-coated hydrophilic environment that encouraged the cells to remain in suspension [42]. Once suspended, the cells were free to aggregate and self-assemble into spheroidal structures. The pellet culture method, on the other hand, forced the cells into a cell pellet that subsequently aggregated and became spheroidal. The suspension culture method is considered to be a less severe method of aggregation with the cells self-aggregating and self-assembling.

Monitoring of the aggregation processes over 48 hours gave the first indication that aggregation technique could hold an influence over subsequent cell behaviour. The suspension culture method initially created multiple small aggregates that eventually joined together to form a single aggregate per well. Similar occurrences were noted when forming suspension culture aggregates using an MLO-A5 cell line [45]. The sometimes elongated and irregular shape of the aggregates formed using this technique suggested that the inner-structure of the final aggregates still comprised the initial small aggregates. The pellet culture method, however, formed a single cell pellet immediately upon centrifugation with, what is suspected to be, a more uniform inner-aggregate structure. This resulted in the final aggregates produced being significantly different in terms of size and, in some cases, shape despite being produced using the same initial cell numbers [Fig. 1].

In terms of HUVEC arrangements, the initial aggregate structure visually appeared to influence cellular arrangement, even prior to the addition of any further culture conditions, i.e. loaded or static culturing. Confocal z-stacking has shown what is thought to be the suspension culture aggregates having an enhanced HUVEC arrangement immediately post-collagen encapsulation compared to the pellet culture aggregates [Fig. 3]. Quantitative data concerning HUVEC distribution, however, has not shown significant differences between either aggregation technique at this early stage. Nevertheless, these early visual observations are thought to further compound the theory that the suspension

aggregates were comprised of multiple small aggregates which later joined together to make up one large aggregate body. The small aggregates making up the final large aggregate offered an inner-aggregate structure that was lacking in the aggregates of the pellet culture method, which is believed to later aid HUVEC arrangement. Saleh and colleagues co-cultured HUVECs with MSCs and demonstrated a similar cellular arrangement to our own [44]. A similar phenomenon was also noted by Stahl et al. who cultured primary osteoblasts with human ECs [46]. Both studies used 50% HUVECs in their co-cultures, with the majority of the HUVECs been seen to be located around the periphery of the aggregates after several days in culture. Uniquely, our study has demonstrated that a low percentage of HUVECs, e.g. 5%, within a co-culture would have a compromised ability to self-organise into arrangements thought to represent pre-vascularisation. However, the application of appropriate culture conditions, e.g. suspension aggregation and hydrostatic loading, could stimulate a low percentage of HUVECs to self-organise into more tissue-like pre-vascular arrangements. One theory put forward to explain this cellular self-assembly is the differential adhesion hypothesis (DAH) [47]. This theory simply states that cells will aggregate to maximise adhesion and minimise energy expenditure with different cell types segregating according to cell – cell adhesion capabilities; those cells of a higher cohesion form the aggregate centre and those with a lower cohesion form the aggregate periphery. It is suspected that if this study was to use as high HUVEC percentages as those previously reported by others [44,46], i.e. 50%, the suspension culture aggregates would maintain similar cellular arrangements as those reported here, but the pellet culture aggregates would have HUVEC-rich peripheral layers, similar to those reported by Saleh [44] and Stahl [46].

Cellular migration from the aggregates into the encapsulating collagen was also observed from the very early stages of the study [Fig. 2]. This phenomenon has been observed previously with other cell types [48,49]. It is theorised that the density gradient between the aggregates and the encapsulating collagen here encouraged the initial outgrowth. Krewson et al. noted that neurite outgrowth was most significant in lower concentration hydrogels, and decreased, thereafter, with increasing concentrations [50]. Thus, one plausible explanation for the onset of the outgrowth observed here is that the surrounding collagen gel was of a lower density than the cellular aggregates. The collagen gel used within this study was 3 mg/ml; similar to that used in a previous study carried out by our laboratory [45]. In our previous study, it was noted that within just 48 hours, the encapsulated, statically-cultured MLO-A5 aggregates became denser than their surrounding collagen. Therefore, it is suggested that the aggregates cultured here too, quickly became denser than their encapsulating collagen; thus, encouraging outgrowth. What is particularly interesting, however, is the observation that the statically-cultured aggregates experienced measurably higher levels of outgrowth compared to their hydrostatically-loaded counterparts. The cellular outgrowth noted from the hydrostatically-loaded samples was visible from the early stages of the study, but ceased to expand as the study progressed. Comparatively, the outgrowth noted from the statically-cultured samples was already significantly more advanced after just three days in culture, and continued throughout the later stages of the study [Fig. 2]. An explanation for these observations is the variance in differentiation rates between the loaded and static cultures. It has been shown previously that hydrostatic loading promotes the proliferation, cytoskeletal assembly [51], and osteogenic differentiation of MSCs [52]. Interestingly, hydrostatic loading, in particular, has been shown to promote such differentiation via the Ras homolog gene family, member A (RhoA) pathway [52], and excessive RhoA activation has been shown to inhibit cellular migration [53,54]. Therefore, one explanation for this outgrowth phenomenon is that the cells of the loaded culture were differentiating at an accelerated rate compared to the cells of the static culture; thus, significantly reducing their migratory capacity. Another plausible explanation for this observed phenomenon could reside with MSCs known ability to act as perivascular precursor cells to influence EC stability. MSCs have been shown to express a panel of cardiac and smooth muscle cell markers that stabilise tubular structures formed by ECs [55], and the enhanced stimulatory effects of the hydrostatically-loaded environment could have augmented this function; thus, reducing migration. The stabilisation capacity of MSCs for ECs was also confirmed by Bourget and colleagues [56]. Further investigation is required, however, to confirm these hypotheses.

Subsequent culture conditions have also been seen to influence inner-aggregate cellular arrangement. That is, there were no significant quantitative differences with regards to HUVEC distribution between any of the experimental conditions after just 3 days. After 10 days, however, both of the loaded sample variables showed decreased HUVEC distribution, whilst both of the static sample variables showed increased HUVEC distribution [Fig. 4B]. That is to say, the HUVECs of the loaded samples appeared more organised, whilst those of the static samples were more homogenously distributed. These data would suggest that hydrostatic loading positively influenced cellular organisation, whilst static culturing did not. This may, in part, be due to VE-cadherin expression. VE-cadherin is present at endothelial adherent junctions and has been reported to play an important role in the intercellular adhesion, differentiation, growth and migration of ECs [57]. The expression of such has also been shown to be upregulated under shear stress conditions [58] making its increased expression under hydrostatic loading a likely contributor to the increased cellular arrangements noted in this study. After 10 days in culture, both of the loaded aggregate variables differed from their statically-cultured counterparts to different degrees. That is to say, hydrostatic loading had a more significant effect on the suspension culture aggregates, compared to the pellet culture aggregate. This may be evidence of a synergistic effect between aggregation technique and the application of hydrostatic loading on levels of cellular arrangement.

It should be noted that whilst the primary focus of this early stage study was to evaluate how specific culture conditions would affect cellular arrangements within 3D aggregated environments, intending to provide a route for improved angiogenic infiltration once implanted, enhancing the integration and subsequent chances of survival for the

graft, it is not without scope for future refinement and progression. Should the study be carried forward to include the assessment of functionality of the possible vascularity, long term *in vivo* implantation would be a minimum requirement. Additionally, cellular outgrowth and the relevance of such for graft viability and possible pre-vascularisation would also be included in any future studies.

Conclusions

In conclusion, clear differences can be seen when comparing aggregate formation techniques and subsequent culture conditions for possible effects on cellular arrangements resembling pre-vascularisation within MSC/HUVEC co-cultured aggregates, when HUVECs are present in the aggregates at very low concentrations. How the aggregates were formed appears to affect the inner-aggregate architecture, which in turn, affects how the HUVECs are arranged within the final cellular aggregate body. The suspension culture aggregates are thought to have had a more compartmentalised inner-structure compared to the more homogeneous inner-structure of the pellet culture aggregates. This increased inner-aggregate structure allowed for a higher degree of cellular arrangement within the aggregates. In addition, culture conditions have been shown to further influence cellular arrangement. The aggregates cultured under hydrostatically-loaded conditions, regardless of aggregate formation technique, experienced a considerably higher level of cellular arrangement compared to those cultured under static conditions. Taking both aggregation method and culture conditions together for the evaluation of cellular arrangements resembling pre-vascularisation, it would appear that the suspension culture aggregates cultured under hydrostatic loading offered the best environment, closely followed by the pellet culture aggregates cultured under hydrostatic loading, the suspension culture aggregates cultured under static conditions, and the pellet culture aggregates cultured under static conditions.

Funding

Financial support was obtained from the Royal Society International Exchange Fund (IE110288) and the NHS Charitable Fund (0011).

Conflicts of interest

The authors declare no conflicts of interest.

Acknowledgments

The authors would like to acknowledge and thank our funding bodies; their support is highly appreciated.

REFERENCES

[1] Liu Y, Chan JKY, Teoh S-H. Review of vascularised bone tissue-engineering strategies with a focus on co-culture systems. J Tissue Eng Regen Med 2015;9:85–105.
[2] Melchiorri AJ, Nguyen B-NB, Fisher JP. Mesenchymal stem cells: roles and relationships in vascularization. Tissue Eng Part B Rev 2014;20:218–28.
[3] Rouwkema J, Rivron NC, van Blitterswijk CA. Vascularization in tissue engineering. Trends Biotechnol 2008;26:434–41.
[4] Lovett M, Lee K, Edwards A, Kaplan DL. Vascularization strategies for tissue engineering. Tissue Eng Part B Rev 2009;15:353–70.
[5] Fuchs S, Hofmann A, Kirkpatrick CJ. Microvessel-like structures from outgrowth endothelial cells from human peripheral blood in 2-dimensional and 3-dimensional co-cultures with osteoblastic lineage cells. Tissue Eng 2007;13:2577–88.
[6] Melero-Martin JM, De Obaldia ME, Kang S-Y, Khan ZA, Yuan L, Oettgen P, et al. Engineering robust and functional vascular networks in vivo with human adult and cord blood-derived progenitor cells. Circ Res 2008;103:194–202.
[7] Fuchs S, Ghanaati S, Orth C, Barbeck M, Kolbe M, Hofmann A, et al. Contribution of outgrowth endothelial cells from human peripheral blood on in vivo vascularization of bone tissue engineered constructs based on starch polycaprolactone scaffolds. Biomaterials 2009;30:526–34.
[8] Tsigkou O, Pomerantseva I, Spencer JA, Redondo PA, Hart AR, O'Doherty E, et al. Engineered vascularized bone grafts. Proc Natl Acad Sci U S A 2010;107:3311–6.
[9] Zhang B, Wu X, Zhang X, Sun Y, Yan Y, Shi H, et al. Human umbilical cord mesenchymal stem cell exosomes enhance angiogenesis through the Wnt4/β-Catenin pathway. Stem Cells Transl Med 2015;4:513–22.
[10] Shabbir A, Cox A, Rodriguez-Menocal L, Salgado M, Badiavas EV. Mesenchymal stem cell exosomes induce proliferation and migration of normal and chronic wound fibroblasts, and enhance angiogenesis in vitro. Stem Cell Dev 2015;24:1635–47.
[11] Zhang J, Guan J, Niu X, Hu G, Guo S, Li Q, et al. Exosomes released from human induced pluripotent stem cells-derived MSCs facilitate cutaneous wound healing by promoting collagen synthesis and angiogenesis. J Transl Med 2015;13:49.
[12] Zhang T, Lee YW, Rui YF, Cheng TY, Jiang XH, Li G. Bone marrow-derived mesenchymal stem cells promote growth and angiogenesis of breast and prostate tumors. Stem Cell Res Ther 2013;4:70–85.
[13] Zigdon-Giladi H, Bick T, Lewinson D, Machtei EE. Co-transplantation of endothelial progenitor cells and mesenchymal stem cells promote neovascularization and bone regeneration. Clin Implant Dent Relat Res 2015;17:353–9.
[14] Prosecka E, Rampichova M, Litvinec A, Tonar Z, Kralickova M, Vojtova L, et al. Collagen/hydroxyapatite scaffold enriched with polycaprolactone nanofibers, thrombocyte-rich solution and mesenchymal stem cells promotes regeneration in large bone defect in vivo. J Biomed Mater Res A 2015;103:671–82.
[15] Elkhenany H, Amelse L, Lafont A, Bourdo S, Caldwell M, Neilsen N, et al. Graphene supports in vitro proliferation and osteogenic differentiation of goat adult mesenchymal stem cells: potential for bone tissue engineering. J Appl Toxicol 2015;35:367–74.
[16] Liu H, Xu GW, Wang YF, Zhao HS, Xiong S, Wu Y, et al. Composite scaffolds of nano-hydroxyapatite and silk fibroin enhance mesenchymal stem cell-based bone regeneration

via the interleukin 1 alpha autocrine/paracrine signaling loop. Biomaterials 2015;49:103–12.
[17] Wang P, Liu X, Zhao L, Weir MD, Sun J, Chen W, et al. Bone tissue engineering via human induced pluripotent, umbilical cord and bone marrow mesenchymal stem cells in rat cranium. Acta Biomater 2015;18:236–48.
[18] Bhang SH, Lee S, Shin J-Y, Lee T-J, Kim B-S. Transplantation of cord blood mesenchymal stem cells as spheroids enhances vascularization. Tissue Eng Part A 2012;18:2138–47.
[19] Laschke MW, Schank TE, Scheuer C, Kleer S, Schuler S, Metzger W, et al. Three-dimensional spheroids of adipose-derived mesenchymal stem cells are potent initiators of blood vessel formation in porous polyurethane scaffolds. Acta Biomater 2013;9:6876–84.
[20] Reinwald Y, Leonard KHL, Henstock JR, Whiteley JP, Osborne JM, Waters SL, et al. Evaluation of the growth environment of a hydrostatic force bioreactor for preconditioning of tissue-engineered constructs. Tissue Eng Part C Methods 2015;21:1–14.
[21] McCoy RJ, O'Brien FJ. Influence of shear stress in perfusion bioreactor cultures for the development of three-dimensional bone tissue constructs: a review. Tissue Eng B Rev 2010;16:587–601.
[22] Burger EH, Klein-Nulend J, Veldhuijzen JP. Mechanical stress and osteogenesis in vitro. J Bone Miner Res Off J Am Soc Bone Miner Res 1992;7:S397–401.
[23] Burger EH, Klein-Nulend J. Mechanotransduction in bone–role of the lacuno-canalicular network. FASEB J Off Publ Fed Am Soc Exp Biol 1999;13:S101–12.
[24] Macdonald AG, Fraser PJ. The transduction of very small hydrostatic pressures. Comp Biochem Physiol A Mol Integr Physiol 1999;122:13–36.
[25] Mullender M, El Haj AJ, Yang Y, van Duin MA, Burger EH, Klein-Nulend J. Mechanotransduction of bone cells in vitro: mechanobiology of bone tissue. Med Biol Eng Comput 2004;42:14–21.
[26] Lelkes G. Experiments in vitro on the role of movement in the development of joints. J Embryol Exp Morphol 1958;6:183–6.
[27] Hosseini A, Hogg DA. The effects of paralysis on skeletal development in the chick embryo. I. General effects. J Anat 1991;177:159–68.
[28] Carter DR, Beaupre GS, Giori NJ, Helms JA. Mechanobiology of skeletal regeneration. Clin Orthop 1998;355:S41–55.
[29] Frieboes LR, Gupta R. An in-vitro traumatic model to evaluate the response of myelinated cultures to sustained hydrostatic compression injury. J Neurotrauma 2009;26:2245–56.
[30] Henstock JR, Rotherham M, Rose JB, El Haj AJ. Cyclic hydrostatic pressure stimulates enhanced bone development in the foetal chick femur in vitro. Bone 2013;53:468–77.
[31] Pörtner R, Nagel-Heyer S, Goepfert C, Adamietz P, Meenen NM. Bioreactor design for tissue engineering. J Biosci Bioeng 2005;100:235–45.
[32] Hanson MA, Ge X, Kostov Y, Brorson KA, Moreira AR, Rao G. Comparisons of optical pH and dissolved oxygen sensors with traditional electrochemical probes during mammalian cell culture. Biotechnol Bioeng 2007;97:833–41.
[33] UC Research Repository, 2007. https://ir.canterbury.ac.nz/handle/10092/2541.
[34] Metzen E, Wolff M, Fandrey J, Jelkmann W. Pericellular PO2 and O2 consumption in monolayer cell cultures. Respir Physiol 1995;100:101–6.
[35] Xu X, Smith S, Urban J, Cui Z. An in line non-invasive optical system to monitor pH in cell and tissue culture. Med Eng Phys 2006;28:468–74.
[36] Malda J, Klein TJ, Upton Z. The roles of hypoxia in the in vitro engineering of tissues. Tissue Eng 2007;13:2153–62.
[37] Wang Y, Wan C, Deng L, Liu X, Cao X, Gilbert SR, et al. The hypoxia-inducible factor alpha pathway couples angiogenesis to osteogenesis during skeletal development. J Clin Invest 2007;117:1616–26.
[38] Volkmer E, Drosse I, Otto S, Stangelmayer A, Stengele M, Kallukalam BC, et al. Hypoxia in static and dynamic 3D culture systems for tissue engineering of bone. Tissue Eng Part A 2008;14:1331–40.
[39] Zhou H, Purdie J, Wang T, Ouyang A. pH measurement and a rational and practical pH control strategy for high throughput cell culture system. Biotechnol Prog 2010;26:872–80.
[40] D'Ippolito G, Diabira S, Howard GA, Menei P, Roos BA, Schiller PC. Marrow-isolated adult multilineage inducible (MIAMI) cells, a unique population of postnatal young and old human cells with extensive expansion and differentiation potential. J Cell Sci 2004;117:2971–81.
[41] Yamawaki H, Pan S, Lee RT, Berk BC. Fluid shear stress inhibits vascular inflammation by decreasing thioredoxin-interacting protein in endothelial cells. J Clin Invest 2005;115:733–8.
[42] Aydin HM, Hu B, Sulé Suso J, El Haj A, Yang Y. Study of tissue engineered bone nodules by Fourier transform infrared spectroscopy. Analyst 2011;136:775–80.
[43] Rouwkema J, de Boer J, Van Blitterswijk CA. Endothelial cells assemble into a 3-dimensional prevascular network in a bone tissue engineering construct. Tissue Eng 2006;12:2685–93.
[44] Saleh FA, Whyte M, Genever PG. Effects of endothelial cells on human mesenchymal stem cell activity in a three-dimensional in vitro model. Eur Cells Mater 2011;22:242–57.
[45] Deegan AJ, Aydin HM, Hu B, Konduru S, Kuiper JH, Yang Y. A facile in vitro model to study rapid mineralization in bone tissues. Biomed Eng Online 2014;13:136–53.
[46] Stahl A, Wenger A, Weber H, Stark GB, Augustin HG, Finkenzeller G. Bi-directional cell contact-dependent regulation of gene expression between endothelial cells and osteoblasts in a three-dimensional spheroidal coculture model. Biochem Biophys Res Commun 2004;322:684–92.
[47] Steinberg MS. On the mechanism of tissue reconstruction by dissociated cells, III. Free energy relations and the reorganization of fused, heteronomic tissue fragments. Proc Natl Acad Sci U S A 1962;48:1769–76.
[48] Seyedhassantehrani N, Li Y, Yao L. Dynamic behaviors of astrocytes in chemically modified fibrin and collagen hydrogels. Integr Biol Quant Biosci Nano Macro 2016;8:624–34.
[49] Sokol ES, Miller DH, Breggia A, Spencer KC, Arendt LM, Gupta PB. Growth of human breast tissues from patient cells in 3D hydrogel scaffolds. Breast Cancer Res BCR 2016;18:19–32.
[50] Krewson CE, Chung SW, Dai W, Mark Saltzman W. Cell aggregation and neurite growth in gels of extracellular matrix molecules. Biotechnol Bioeng 1994;43:555–62.
[51] Zhang H, Dai S, Bi J, Liu K-K. Biomimetic three-dimensional microenvironment for controlling stem cell fate. Interfac Focus 2011;1:792–803.
[52] Zhao Y-H, Lv X, Liu Y-L, Zhao Y, Li Q, Chen Y-J, et al. Hydrostatic pressure promotes the proliferation and osteogenic/chondrogenic differentiation of mesenchymal stem cells: the roles of RhoA and Rac1. Stem Cell Res 2015;14:283–96.
[53] Arthur WT, Burridge K. RhoA inactivation by p190RhoGAP regulates cell spreading and migration by promoting membrane protrusion and polarity. Mol Biol Cell 2001;12:2711–20.

[54] Cox EA, Sastry SK, Huttenlocher A. Integrin-mediated adhesion regulates cell polarity and membrane protrusion through the Rho family of GTPases. Mol Biol Cell 2001;12:265–77.
[55] Au P, Tam J, Fukumura D, Jain RK. Bone marrow-derived mesenchymal stem cells facilitate engineering of long-lasting functional vasculature. Blood 2008;111:4551–8.
[56] Bourget Jean-Michel, Kérourédan Olivia, Medina Manuela, Rémy Murielle, Thébaud Noélie Brunehilda, Bareille Reine, et al. Patterning of endothelial cells and mesenchymal stem cells by laser-assisted bioprinting to study cell migration. BioMed Res Int 2016;3569843.
[57] Yamamoto K, Takahashi T, Asahara T, Ohura N, Sokabe T, Kamiya A, et al. Proliferation, differentiation, and tube formation by endothelial progenitor cells in response to shear stress. J Appl Physiol 2003;95:2081–8.
[58] Noria S, Cowan DB, Gotlieb AI, Langille BL. Transient and steady-state effects of shear stress on endothelial cell adherens junctions. Circ Res 1999;85:504–14.